New cobalt-based metal-organic frameworks for catalysing sulfite in degradation of reactive brilliant red

Yi-Ru Zhang,[a] Yan-Bing, Liang,[a] Dan Jian,[a] Jian-Zhong Wu,*[b] and Yong-Cong Ou*[a]

a *Guangdong Provincial Key Laboratory of Carbon Dioxide Resource Utilization, School of Chemistry, South China Normal University, Guangzhou 510006, China. Email: ouyongcong@m.scnu.edu.cn*

b *Key Laboratory of Theoretical Chemistry of Environment, Ministry of Education, School of Chemistry, South China Normal University, Guangzhou 510006, China. Email: wujzh@scnu.edu.cn*

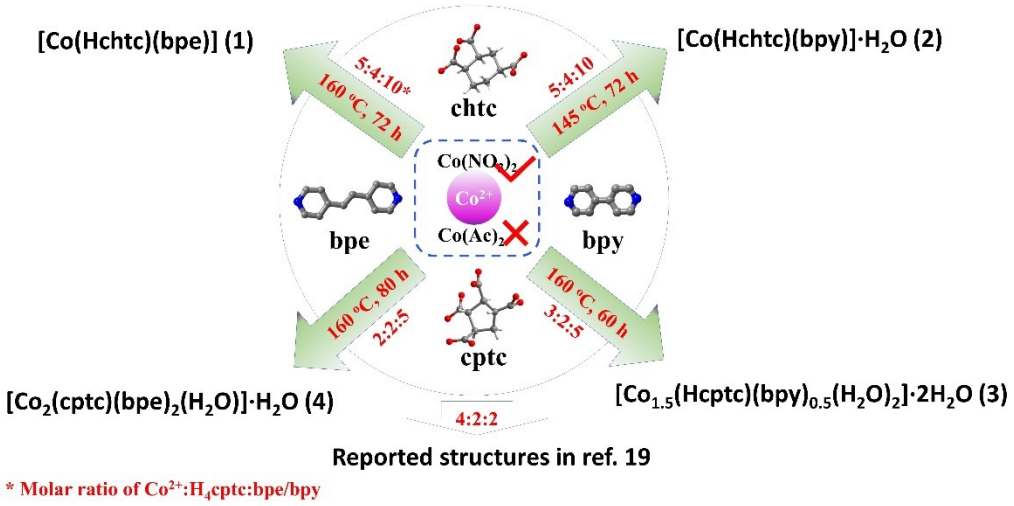

Figure S1. The reaction scheme for the four structures in different synthetic conditions.

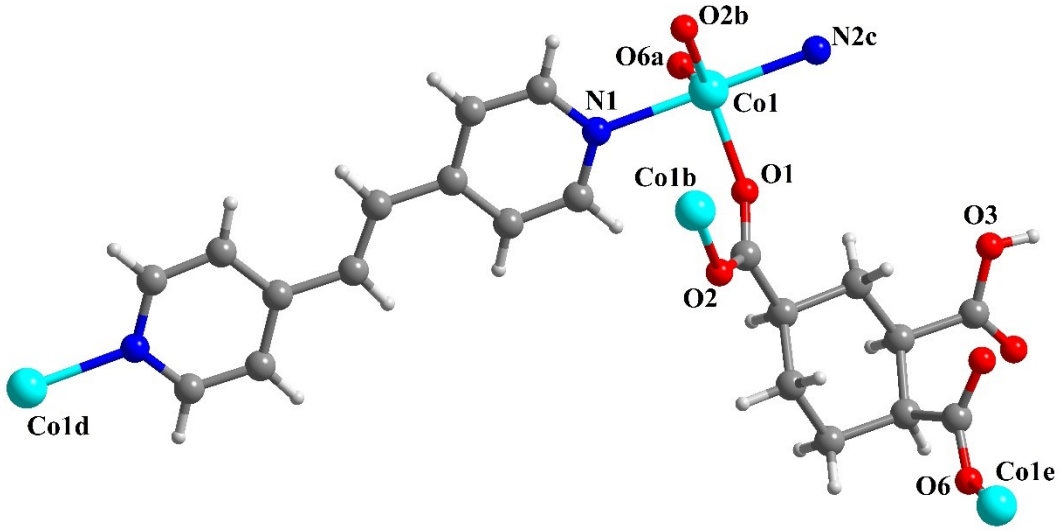

Figure S2. The coordination environment in asymmetric unit of **1**.

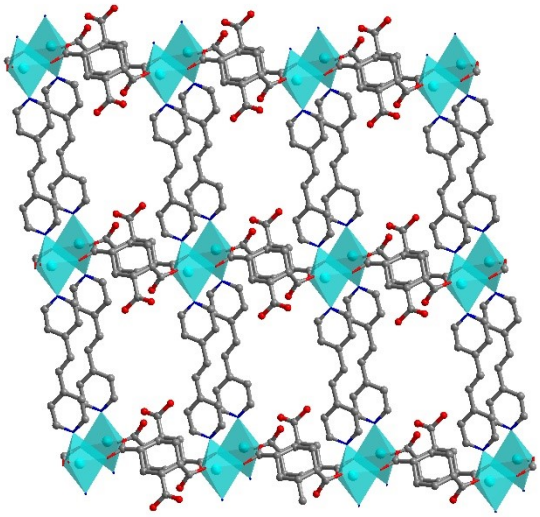

Figure S3. Polyhedral view of two dimensional coordination framework of **1** as double-side brick wall.

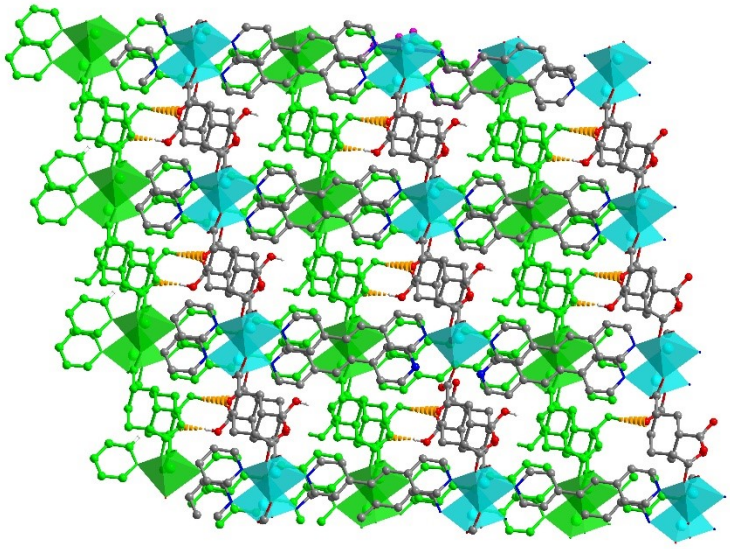

Figure S4. The hydrogen bonding interaction between the two layers of **1**.

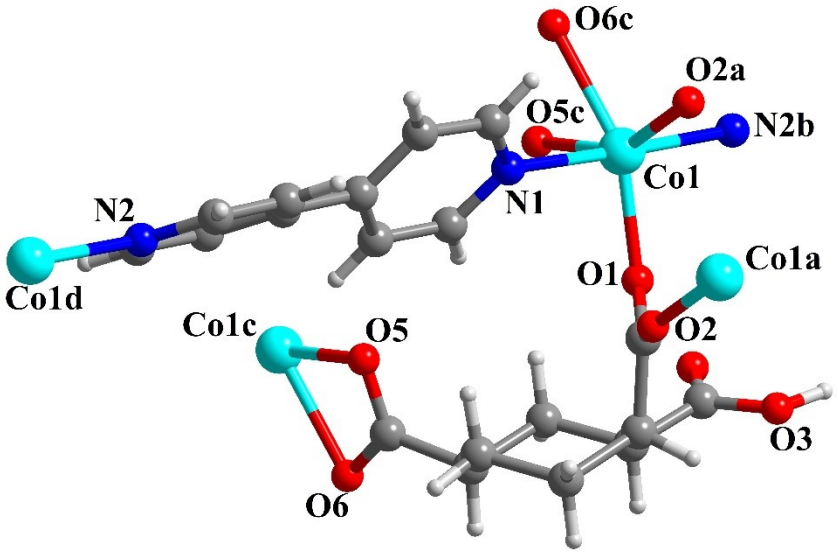

Figure S5. The coordination environment in asymmetric unit of **2**.

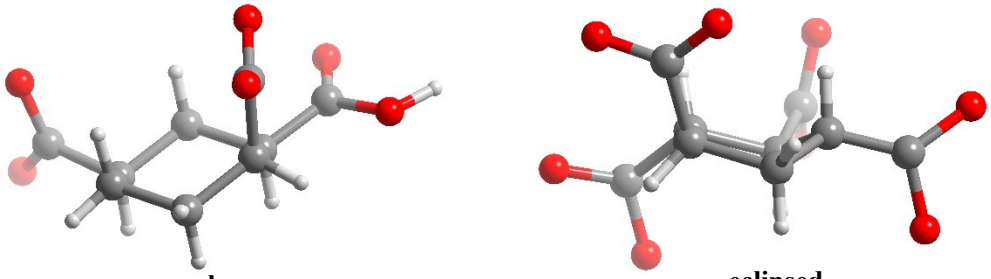

Figure S6. The different conformations for Hchtc (left) and Hcptc (right) ligands.

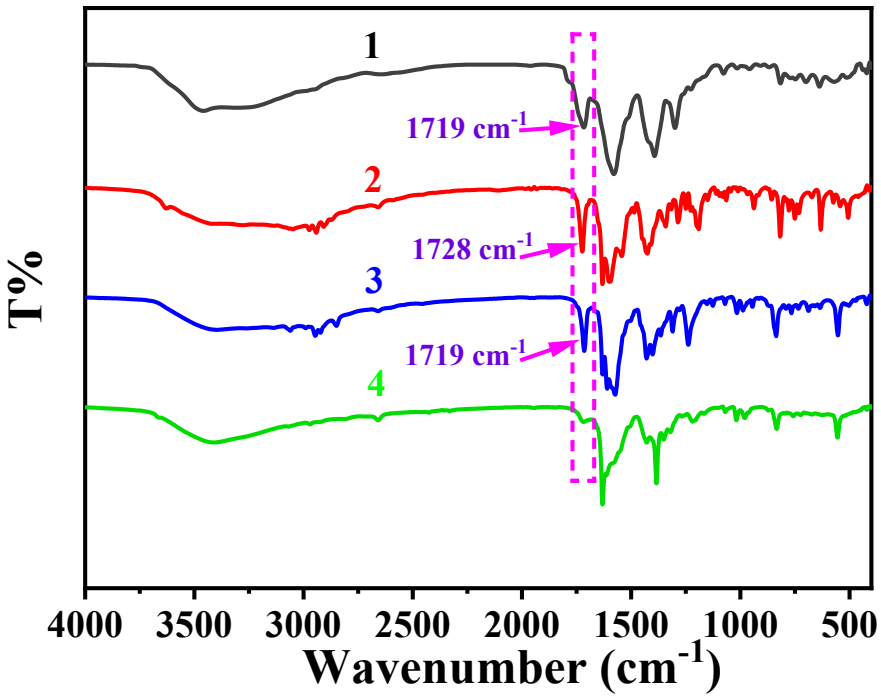

Figure S7. The FTIR spectra for **1-4**, in which the strong absorption peak at about 1720 cm^{-1} is relative to the stretching vibration of –COOH group.

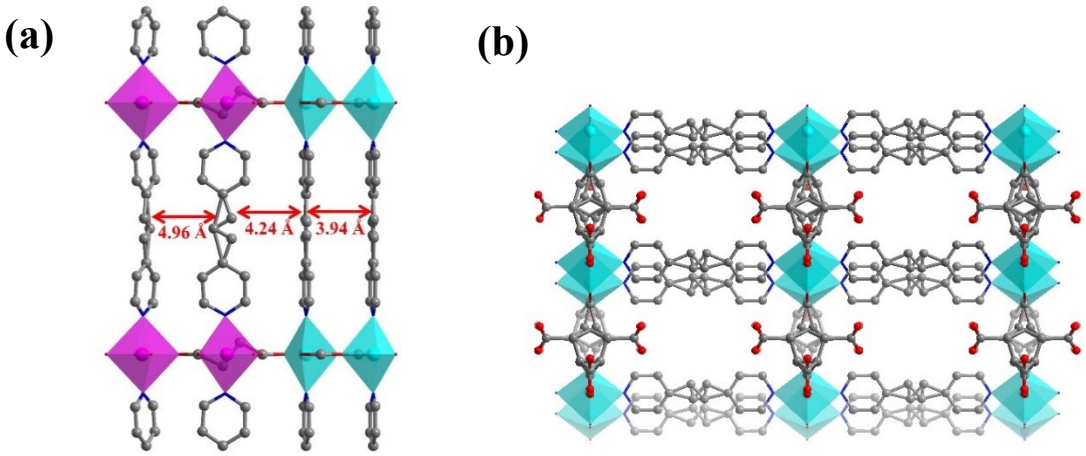

Figure S8. (a) The distances among the bpe ligands in different positions, (b) the coordination layer constructed from dinuclear units and bpe ligands for **4**, which is similar to the layer frameworks in **1** and **2**.

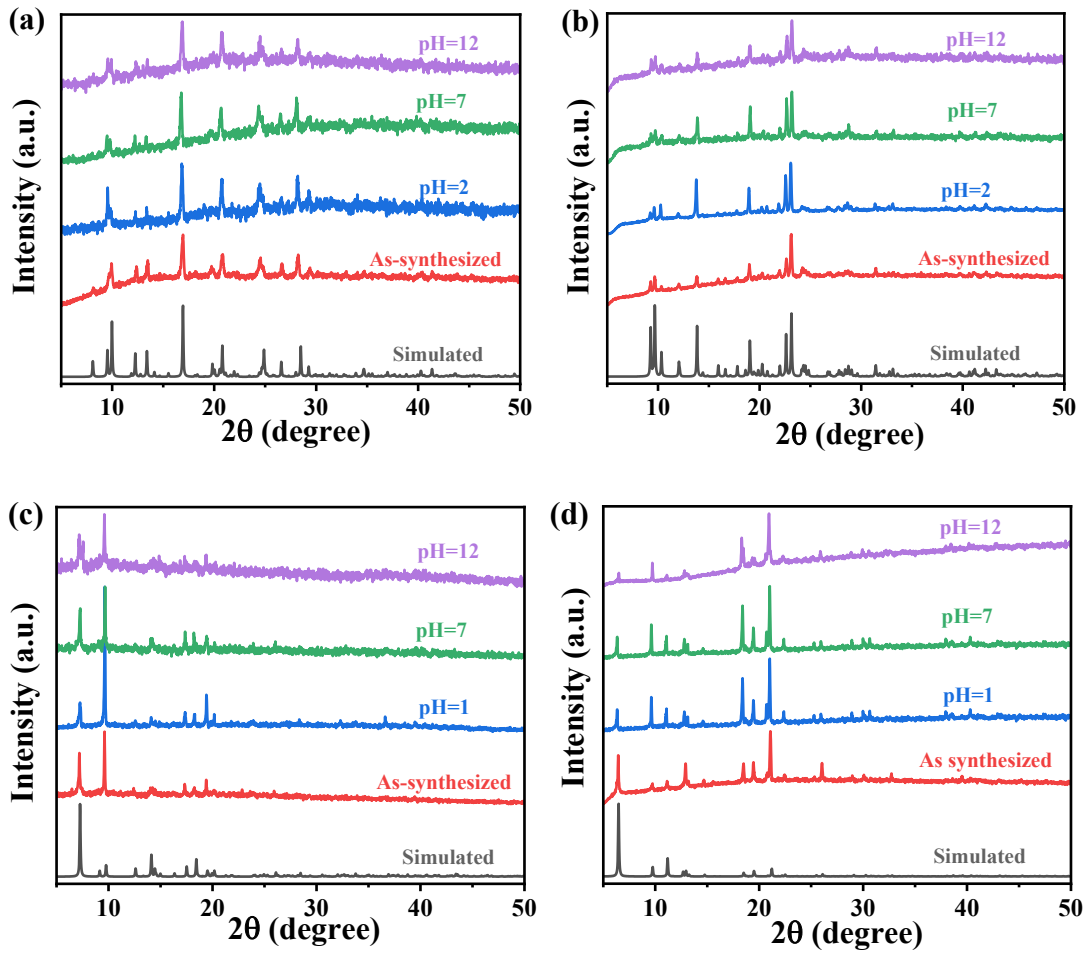

Figure S9. PXRD patterns of the as-synthesized sample and the samples immerged in solutions with different pH values for **1** (a), **2** (b), **3** (c) and **4** (d) respectively.

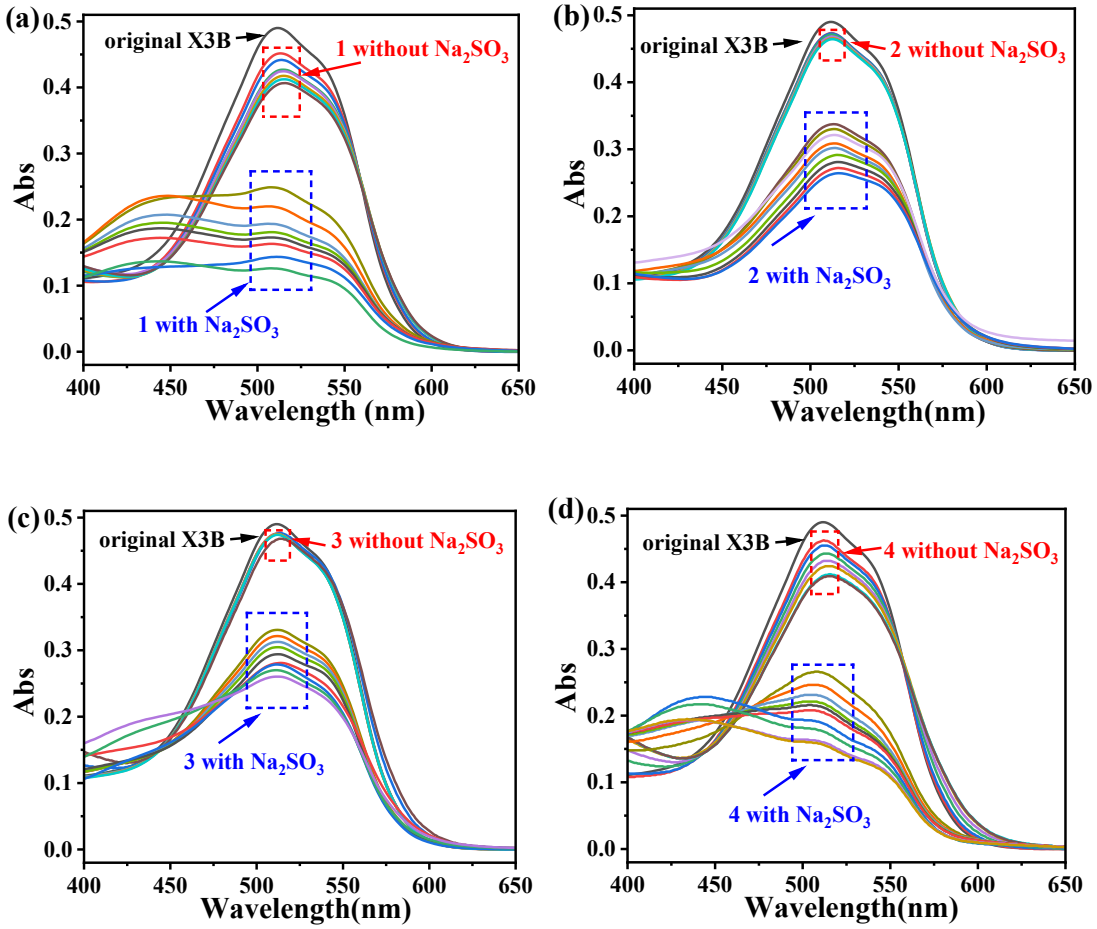

Figure S10. UV-Vis adsorption spectra of the time-dependent adsorption (red dash frame) and degradation (blue dash frame) of X3B for **1** (a), **2** (b), **3** (c) and **4** (d). From top to bottom, the lines within the frames correspond to the curves from 10 min to 150 min.

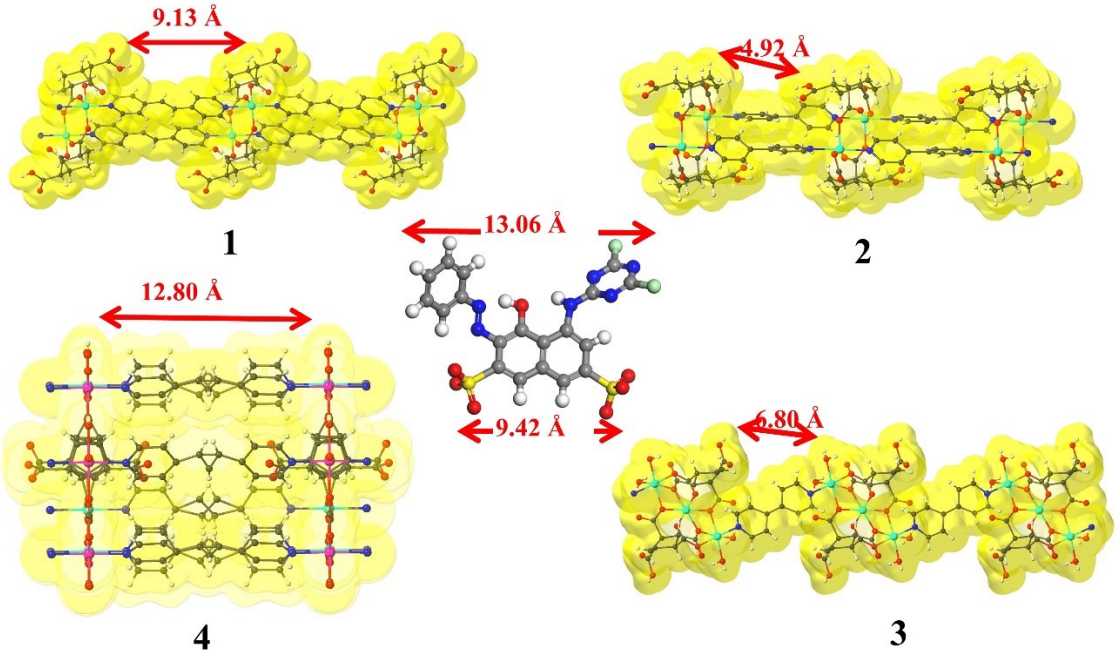

Figure S11. The molecular size of X3B, and the distances between the two metallic units separated by the bpe ligand in **1** and **4**, and the 4,4'-bpy ligands in **2** and **3**.

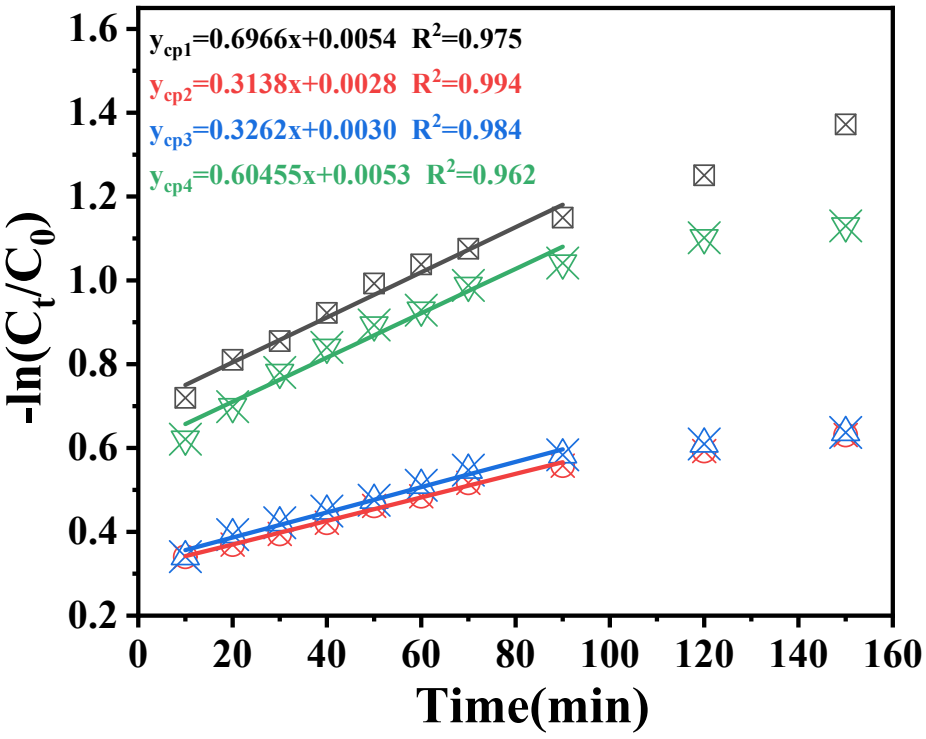

Figure S12. The time-dependent degradation of X3B for **1-4** fitted by pseudo-first-order simulation.

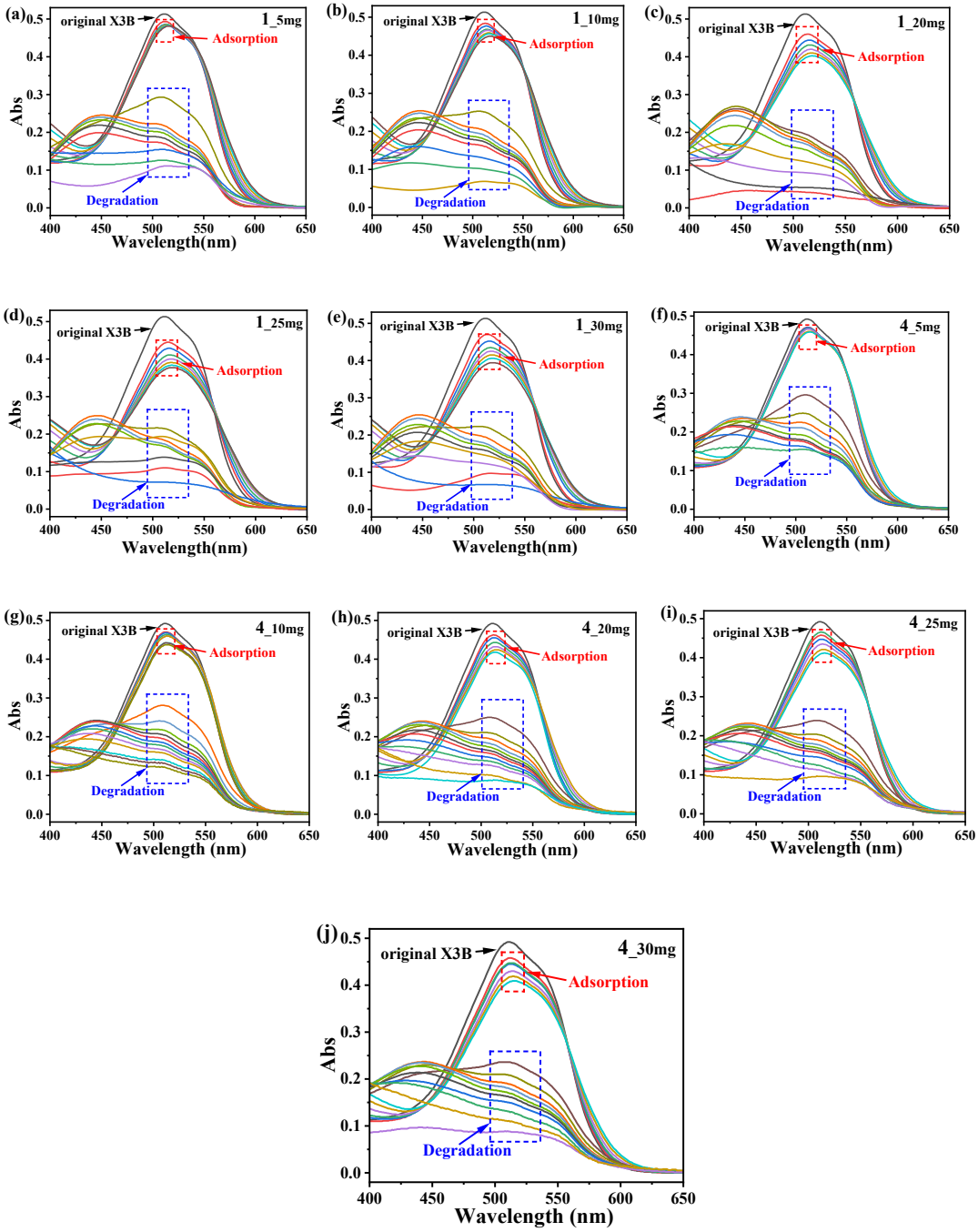

Figure S13. UV-Vis adsorption spectra of the time-dependent adsorption and degradation of X3B for **1** (a-e) and **4** (f-j) in different addition amounts. From top to bottom, the lines within the frames correspond to the curves from 10 min to 150 min.

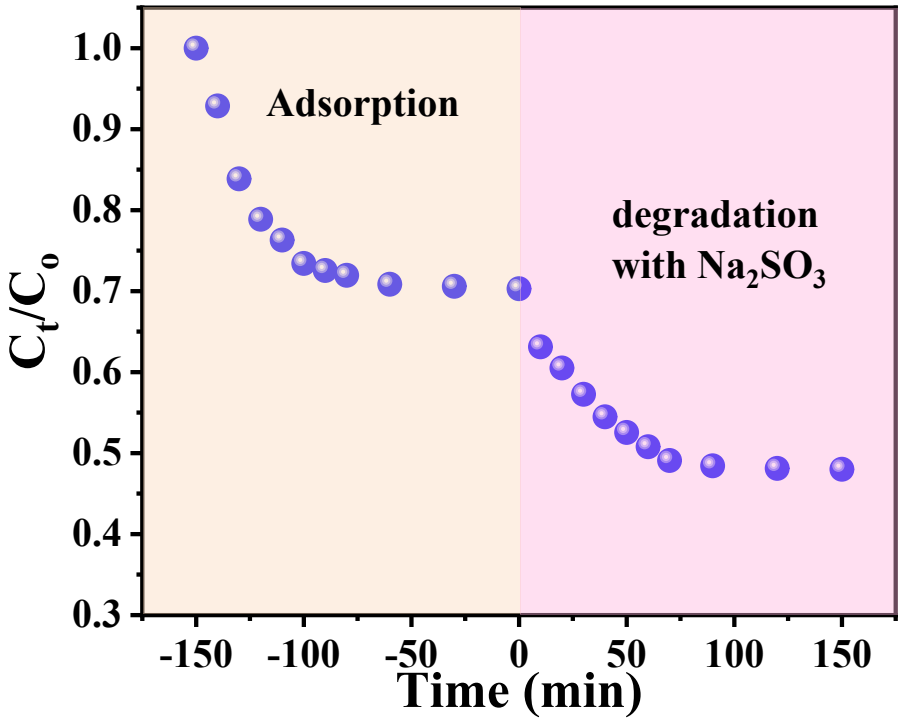

Figure S14. The adsorption and degradation of X3B for the documented crystal $[Co_2(cptc)(bpe)_{0.5}(H_2O)_2]\cdot 2H_2O$.

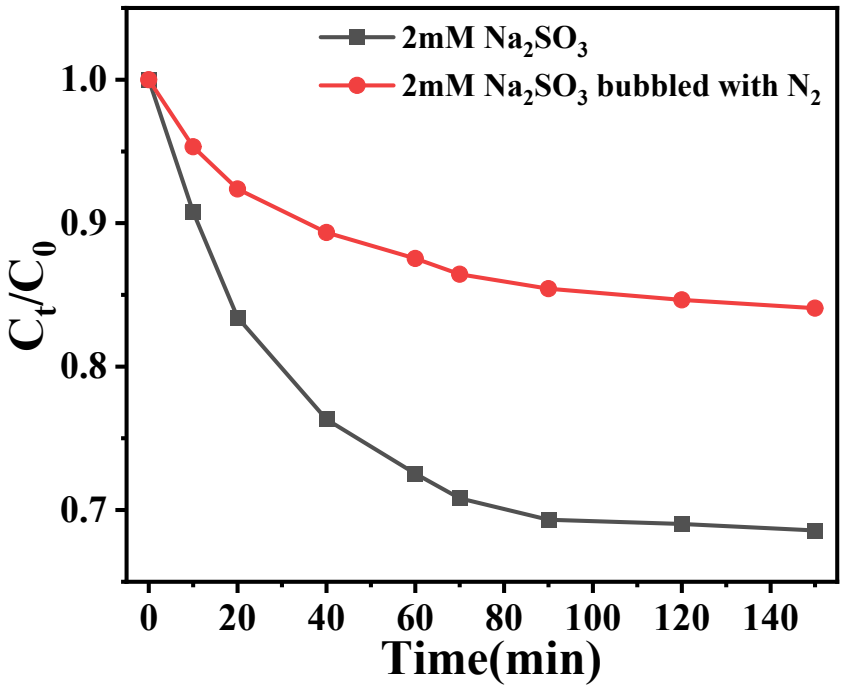

Figure S15. The degradation of X3B in 2 mM Na_2SO_3 solution can be depressed under the N_2 atmosphere.

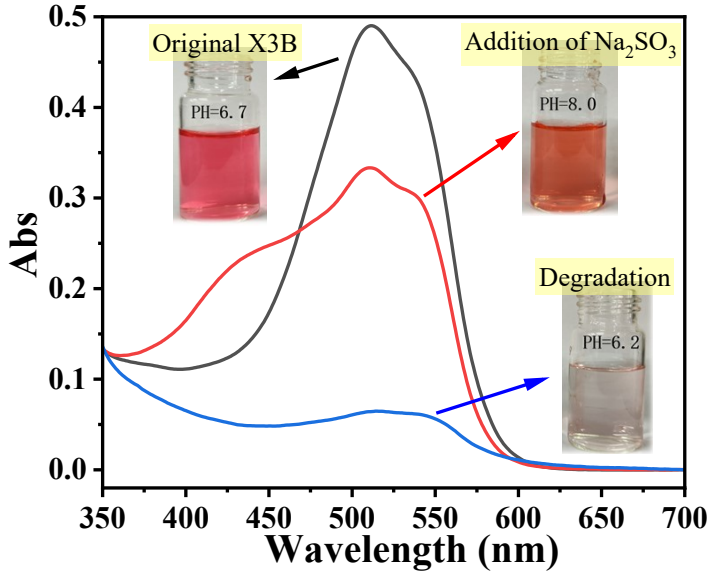

Figure S16. The differences of UV-vis absorption and colors of X3B solution during the degradation.

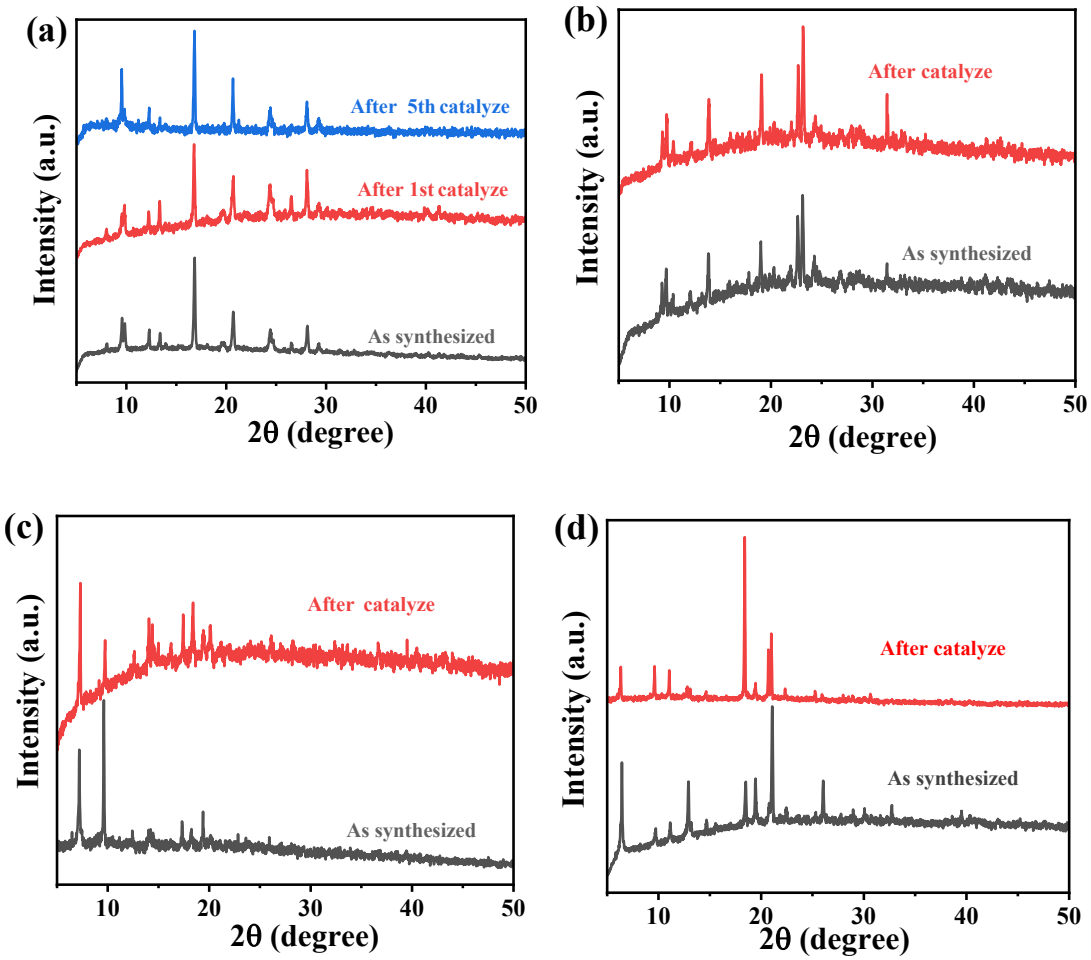

Figure S17. PXRD patterns after catalytic measurements of samples **1** (a), **2** (b), **3** (c) and **4** (d).

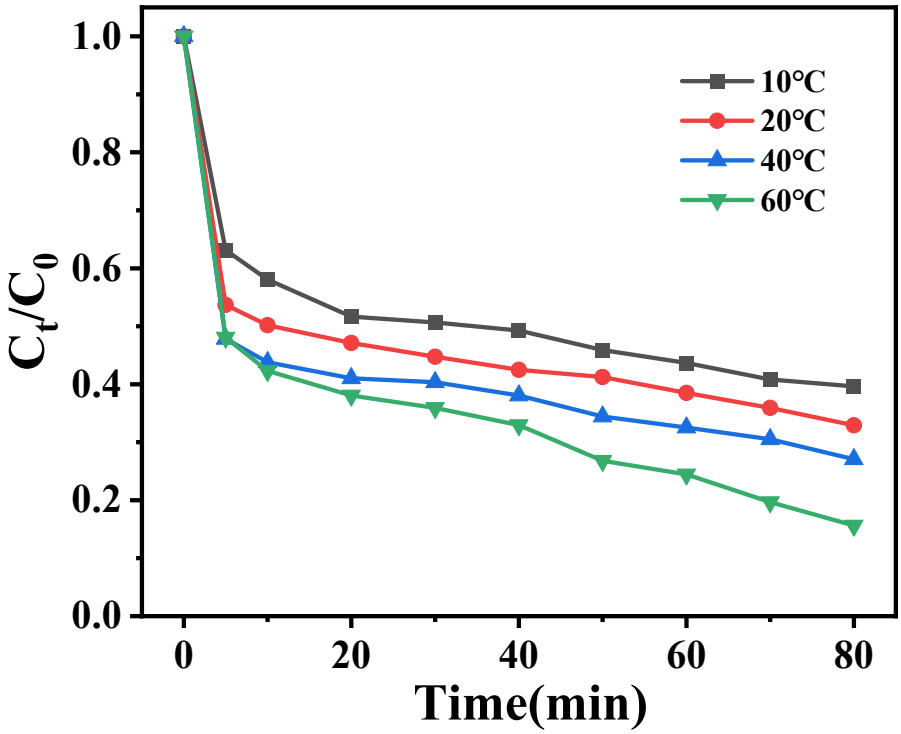

Figure S18. The different degradation of X3B in various temperatures for **1** (X3B, 20 mg/L; Na_2SO_3, 2 mM; **1**, 5 mg).

Table S1. Overview of materials in degradation of X3B through AOPs.

Materials	Catalytic efficiency (%)	Reaction conditions						Reference
		Dosage of catalyst	C_{X3B}	Oxidant / Radical	Temp. (K)	Energy	pH	
$FePz(dtnCl_2)_4$	97%	0.4 mg	0.1 mM	H_2O_2/•OH	303	500 W halogen lamp	2	***S1***
Cadmium borophosphate	90%	167 mg	40 ppm	H_2O_2/•OH	R.T.	Mercury lamp(375W)	-	***S2***
Steel slag	79.2%	10 g/L	20 mg/L	$S_2O_8^{2-}$/$SO_4^{\bullet-}$	R.T.	Sunlight	5.6	***S3***
E/Co(II)/S(IV) system	95.14%	10 μM	30 mg/L	Na_2SO_3/$SO_4^{\bullet-}$	R.T.	Electrical	7-9	***S4***
Gas sludge - S900	90%	2 g	61 mg/L	H_2O_2/•OH	R.T.	Electrical	3	***S5***
NH_4NO_3	94%	1.0 M	50 mg/L	H_2O_2/•OH	R.T.	Electrical	-	***S6***
Fe^0	74.1%	0.2 mM	20 mg/L	Na_2SO_3/$SO_4^{\bullet-}$	R.T.	None	6	***S7***
CuFe@C composite	98%	0.05 g/L	50 mg/L	PMS/$SO_4^{\bullet-}$ and •OH	R.T.	None	7	***S8***
1	90%	20 mg	20 mg/L	Na_2SO_3/$SO_4^{\bullet-}$	R.T.	None	7	***This work***
4	81%	20 mg	20 mg/L	Na_2SO_3/$SO_4^{\bullet-}$	R.T.	None	7	

Table S2. Crystal data and structure refinements for **1-4**.

	1 (150 K)	**2** (293 K)	**3** (150 K)	**4** (150 K)
empirical formula	$C_{21}H_{20}N_2O_6Co$	$C_{19}H_{20}N_2O_7Co$	$C_{14}H_{18}NO_{12}Co_{1.5}$	$C_{33}H_{28}N_4O_9Co_2$
M	455.32	447.30	480.69	742.45
wavelength (Å)	0.71073	1.54178	0.71073	1.54178
crystal system	Triclinic	Monoclinic	Triclinic	Orthorhombic
space group	P1	P1	P1	*Pbam*
a/Å	9.1990(8)	9.5570(6)	7.2508(6)	27.8698(9)
b/Å	9.6032(10)	10.0876(7)	10.4687(11)	9.5761(3)
c/Å	10.9409(10)	10.4840(7)	12.7942(10)	13.6522(4)
α/°	91.168(2)	112.632(7)	72.323(4)	90
β/°	94.667(2)	96.062(6)	89.396(3)	90
γ/°	104.944(2)	98.241(6)	75.982(3)	90
Vol/Å^3	930.19(15)	908.86(11)	895.66(14)	3643.6(2)
Z	2	2	2	4
ρ_{calcd}/g cm^{-3}	1.626	1.634	1.782	1.353
μ/mm^{-1}	0.967	7.833	1.473	7.598
reflns collected	7318	4188	5593	23630
unique reflns	3510(0.0520)	2779(0.0338)	3247(0.0399)	3485(0.1047)
S	1.040	0.938	1.078	1.047
R_1[a], wR_2[b] ($I > 2\sigma(I)$)	0.0695, 0.1776	0.0414, 0.0979	0.0747, 0.2038	0.0769, 0.1953 (squeeze)
R_1[a], wR_2[b] (all data)	0.1296, 0.2292	0.0498, 0.1002	0.1093, 0.2527	0.1019, 0.2164 (squeeze)

[a] $R_1 = \sum||F_o|-|F_c||/\sum|F_o|$, [b] $wR_2 = [\sum w(F_o^2-F_c^2)^2/\sum w(F_o^2)^2]^{1/2}$

Table S3. The hydrogen bonding list for **1**, **2**, **3** and **4**.

D-H...A	d(D-H)	d(H...A)	d(D...A)	<(DHA)
		1		
O(3)-H(3O)...O(5)	0.84	1.83	2.668(7)	171.3
		2		
O(1W)-H(1WA)...O(6)	0.82	1.90	2.703(4)	165.6
O(3)-H(3O)...O(1W)	0.95	1.74	2.691(4)	174.2
C(10)-H(10A)...O(5)	0.93	2.63	3.343(4)	134.0
C(14)-H(14A)...O(3)	0.93	2.61	3.282(4)	129.8
C(16)-H(16A)...O(4)	0.93	2.61	3.316(5)	133.0
C(17)-H(17A)...O(5)	0.93	2.52	3.117(4)	122.1
C(18)-H(18A)...O(2)	0.93	2.35	2.936(4)	120.5
		3		
O(1W)-H(1WA)...O(6)	0.64	2.07	2.708(7)	173.2
O(1W)-H(1WB)...O(4)	0.85	1.88	2.573(14)	137.6
O(2W)-H(2WA)...O(2)	0.85	1.99	2.730(10)	145.0
		4		
O(1W)-H(1WA)...O(6)	0.78	1.92	2.695(7)	176.4
O(1W)-H(1WB)...O(1)	0.78	1.93	2.617(7)	146.7

Reference:

S1. Z. Zhang, Q. Peng, J. Sun, L. Fang and K. Deng, Ind. Eng. Chem. Res., 2013, **52**, 13342–13349.

S2. Y. Feng, L. Lv, D. Bi, Z. Zhong, J. Li, Z. Yue, Z. Zeng, S. Zhang and Z. Meng, CrystEngComm, 2022, **24**, 479-483.

S3. Z. Wang, Y. Guo, Y. Chen, S. Liang, J. Zuo and X. Yu, J. Environ. Eng., 2016, **142**, 04015048.

S4. Y. Ji, W. Li, W. Cao, Z. Yang, C. Zheng and W. Zhang, J. Environ. Chem. Engin., 2024, **12**, 112792.

S5. L. Zhou, Y. Xiao, J. Liang, D. Tang and J. Sun, Emerg. Contam., 2019, **5**, 61-69.

S6. S. Qiu, L. Yu, D. Tang, W. Ren, K. Chen and J. Sun, Ind. Eng. Chem. Res., 2018, **57**, 4907–4915.

S7. P. Xie, Y. Guo, Y. Chen, Z. Wang, R. Shang, S. Wang, J. Ding, Y. Wan, W. Jiang and J. Ma, Chem. Eng. J., 2017, **314**, 240–248.

S8. D. Zhao, W. Fan, Z. Wang, F. Tian, K. Xie, G. Liu, J. Liu, Y. Li and B. L. Li, Sep. Purif. Technol. 2024, **343**, 126997.